

Estimation of the Agulhas ring impacts on meridional heat fluxes and transport using ARGO floats and satellite data

J. M. A. C. Souza,¹ C. de Boyer Montégut,¹ C. Cabanes,² and P. Klein³

Received 19 August 2011; revised 29 September 2011; accepted 30 September 2011; published 1 November 2011.

[1] A method that combines vertical profiles from the ARGO floats program and satellite Sea Surface Height (SSH) data is used to reconstruct the vertical structure of the Agulhas rings. All eddies shed by the Agulhas retroflection in the period between January 2005 and December 2008 were successfully reconstructed. The velocity structures obtained are tilted and phase shifted in relation to the temperature anomalies, resulting in an annual mean eddy meridional heat flux across the ring paths of 0.062 ± 0.012 PW (northward). A first order estimate indicates 0.07 PW entering the Atlantic from the Indian Ocean through Agulhas rings. The volume transport by Agulhas rings is believed to play a central role in the overturning circulation, being the main process responsible for the leakage of Indian Ocean waters to the Atlantic. The new estimates of the [time mean] ring volume transport of 9 ± 8 Sv from the Indian to the Atlantic Ocean fall in the range obtained by previous works. These estimates include a better representation of the trapped water region in the eddies. A large inter-annual variability in the volume transport was observed, with a maximum of ~ 11 – 21 Sv in 2007. This variability is related to the number of structures shed by the Agulhas retroflexion per year. The ring shapes play a secondary, though important, role. **Citation:** Souza, J. M. A. C., C. de Boyer Montégut, C. Cabanes, and P. Klein (2011), Estimation of the Agulhas ring impacts on meridional heat fluxes and transport using ARGO floats and satellite data, *Geophys. Res. Lett.*, 38, L21602, doi:10.1029/2011GL049359.

1. Introduction

[2] The Agulhas rings are the largest mesoscale eddies in the world and play an important role in the transport of Indian Ocean waters to the South Atlantic [*Biastoch et al.*, 2008]. Currently, it is believed that virtually all the upper layer overturning circulation in the Atlantic is originated from Indian Ocean leakage through Agulhas rings. Several studies used satellite altimetry to estimate the Agulhas rings general characteristics and pathways in the South Atlantic [e.g., *Dencausse et al.*, 2010]. But since the altimetry is restricted to the surface, the transport calculations are usually based on numerical model results or simple assumptions about the ring geometry. The lack of *in situ* data makes it difficult to quantify the water trapped by the structures and their temperature and salinity anomalies (T and S, hereinafter). Although several studies [e.g., *van Aken et al.*, 2003; *Schmid et al.*,

2003] have observed the Agulhas rings at sea, such observations are usually restricted to newly formed eddies and do not represent the vertical structure modifications along their lifetimes. In fact, the observed diameter and amplitude modifications along their life cycles have an important impact in the eddy fluxes.

[3] With the advent of the ARGO profiling floats program, a considerable growth in the information about the oceanic vertical structure was observed. Despite the difficulties inherent in observing mesoscale features from Lagrangian data, it is possible to reconstruct the mean eddy vertical structure through the combination of the floats profiles and satellite altimeter data. As an example, *Qiu and Chen* [2005] applied this approach to reevaluate the eddy heat fluxes in the North Pacific.

[4] The objective of the present work is, for the first time, to use the *in situ* data from the ARGO profiling floats to estimate the vertical structure of the Agulhas rings and calculate the associated meridional heat flux and volume transports. The ideas presented by *Qiu and Chen* [2005] are revisited, combining an eddy tracking method based on the Sea Surface Height (SSH) satellite data with vertical profiles from the ARGO program.

2. Data and Methods

2.1. Data

[5] Four years (from January 2005 to December 2008) of SSH data from the AVISO reference product were used. This dataset consists of a merged satellite product, projected on a $1/3^\circ$ horizontal resolution Mercator grid every 7 days [*Le Traon et al.*, 2003]. Sea Level Anomalies (SLA) were obtained by subtracting from the SSH its temporal mean value in each grid point. Seasonal and interannual signals were removed from the SLA data by subtracting the low pass filtered signal (Hanning with a window of 175 days). A Lanczos spatial filter was then applied to eliminate variability with length scales larger than 1000 km.

[6] Vertical profiles from the ARGO program were used to reconstruct the vertical structure of the identified eddies. The ARGO program consists of free-drifting profiling floats that measure T and S in the upper 2000 m of the water column. Only the first 1500 m are considered in the present study due to data inconsistencies in deeper layers. Further details about the ARGO program and access to the data can be obtained at <http://www.ARGO.ucsd.edu/>. In the present case, the re-qualified ARGO data from the CORA (Coriolis Ocean database for Re-Analysis) dataset [*Cabanes et al.*, 2010] are used. To obtain the anomalies from the ARGO profiles, mean fields based on the ARIVO climatology [*von Schuckmann et al.*, 2009] interpolated to the profile positions were used. These mean fields were constructed to

¹Laboratoire d'Océanographie Spatiale, IFREMER, Plouzané, France.

²DT-INSU, IFREMER, Plouzané, France.

³Laboratoire de Physique des Océans, IFREMER, Plouzané, France.

represent the time mean over the same period as SSH and floats datasets (2005–2008).

2.2. Eddies Identification and Tracking

[7] SLA contours were used to detect eddies through a modified winding-angle method. Each eddy is defined as a maximum SLA modulus (eddy center) encircled by a closed contour (eddy edge). In the present study, we applied the algorithm described by *Chaigneau et al.* [2009]. The eddy identification was carried out in two steps: (1) the identification of local SLA modulus maximum corresponding to the eddy centers and (2) the selection of closed SLA contours associated to each eddy. The outermost contour embedding only one eddy center was considered as the eddy edge. This method is very similar to the one applied by *Chelton et al.* [2011], and showed a good performance when compared to other classical methods [*Souza et al.*, 2011]. The eddy diameter is defined as the diameter of a circle with the same area as the polygon defined by the outer SLA contour belonging to the eddy. The eddy amplitude is the modulus of the difference between the maximum SLA inside the eddy and the SLA at its border. After identification, each structure is tracked for its continuation in time. Thus, one eddy (e_1) observed at one time step is compared to another eddy (e_2) identified in the subsequent time step through a dissimilarity parameter (1) proposed by *Penven et al.* [2005].

$$X_{e_1, e_2} = \sqrt{\left(\frac{\Delta X}{X_0}\right)^2 + \left(\frac{\Delta R}{R_0}\right)^2 + \left(\frac{\Delta \xi}{\xi_0}\right)^2} \quad (1)$$

where ΔX is the distance between the centers of the eddies e_1 and e_2 , ΔR is the diameter difference and $\Delta \xi$ their vorticity difference. Characteristic scales for the eddy distance ($X_0 = 1000$ km), diameter ($R_0 = 100$ km) and vorticity ($\xi_0 = 10^{-6}$ s $^{-1}$) are used. X_{e_1, e_2} is calculated for all the rings (e_2) that have the same vorticity sign and are less than 2° distant from e_1 . The ring e_2 that present the minimum value of X_{e_1, e_2} is assumed as the continuation of the eddy e_1 . The algorithm searches for the continuation of the structures for 3 consecutive time steps (3 weeks).

2.3. Vertical Structure Reconstruction

[8] Using the data described above, and adopting some basic assumptions, a mean vertical structure of Agulhas rings is reconstructed. A detailed description of the method is available in the auxiliary material.¹ For each altimetry map, all ARGO profiles that fall into a ± 2 days interval and that are located less than 2.5° (~ 270 km) apart from an eddy center are selected for the reconstruction. The profiles are projected into a zonal axis in function of their distance from the eddy center. The symmetry in the meridional direction is assumed. As eddies are located every 7 days from SLA maps, in the case of profiles that are not from the same instant of the SLA data, the eddy position is linearly interpolated to the time of the ARGO profile for the estimation of its distance from the eddy center.

[9] The present method is similar to the one used by *Qiu and Chen* [2005] to study the eddy heat flux in the subtropical North Pacific. These authors consider that the same

eddy vertical structure was surveyed by all the profiles, ignoring variations with time. This is not the case in the present study, since the Agulhas rings experience important modifications during their trajectories in the South Atlantic. Changes in eddy diameter and amplitude were observed by several authors [e.g., *Schonten et al.*, 2000; *van Sebille et al.*, 2010]. Since ARGO profiles from distinct stages of the eddy life cycles are used, the T and S anomalies and the distances from the eddy center are normalized by the eddy amplitudes and diameters, respectively (2).

$$D_e = \frac{D_p}{\Phi}, (T_e, S_e) = \frac{(T_p, S_p)}{A} \bar{A} \quad (2)$$

where D_e and (T_e, S_e) are the equivalent distance, T and S anomalies; D_p and (T_p, S_p) are the ARGO profile distance from the eddy center and its observed T and S anomalies; Φ and A are the eddy instantaneous diameter and amplitude. The overline indicates the mean value along the eddy life cycle. The linear normalization is based on the fact that a linear relation is observed between the vertical mean T from the ARGO profiles and the eddy amplitudes obtained from the altimetry. Although previous work demonstrated that the amplitude decay of the Agulhas rings is not linear, the relation between the T and S anomalies and the amplitude is constant in time. The eddy section was obtained by fitting, at each depth layer, the equivalent T and S anomalies and distances in the horizontal to a 7th degree Lagrange polynomial. The polynomial was chosen to represent the approximate Gaussian characteristic of the anomaly distribution in the depth layers. The normalization and fitting processes are essential to obtain the vertical structure of the long-lived Agulhas rings. Tests conducted without these processes and using kriging interpolation led to noisy vertical sections that resulted in dynamical heights that do not resemble the SLA obtained from the satellite.

3. Results

[10] From the automatic algorithm, 16 Agulhas rings with durations larger than 6 months were identified (Figure 1a). It was possible to reconstruct all the ring vertical structures. Their general characteristics presented in Table 1 show a good agreement with previous work, which state that a “typical” Agulhas ring is shed every 2–3 months and has a diameter of 150–200 km [*van Sebille et al.*, 2010; *van Aken et al.*, 2003]. The mean propagation velocity is in the range of previous works. Typical values range between 0.05 and 0.09 ms $^{-1}$ [*Garzoli et al.*, 1999]. Table 1 also presents the number of ARGO profiles available for the reconstruction of the eddy vertical structures. The number of profiles per eddy varies between 11 and 93, enabling the volume and heat flux estimates for all Agulhas rings observed in the study period. Further details about the automatic identification and tracking results are given by *Souza et al.* [2011].

[11] To present the results of the vertical structure reconstruction method, an Agulhas ring first observed by the geometric identification method in 24 January 2007, and that traveled for ~ 3772 km across the South Atlantic basin in 791 days, is taken as an example. (The vertical T and S sections of all identified rings are available in the auxiliary material. In these figures, the black contours are the eddy velocities, with intervals of 0.05 ms $^{-1}$.) Figure 1b presents a

¹Auxiliary materials are available in the HTML. doi:10.1029/2011GL049359.

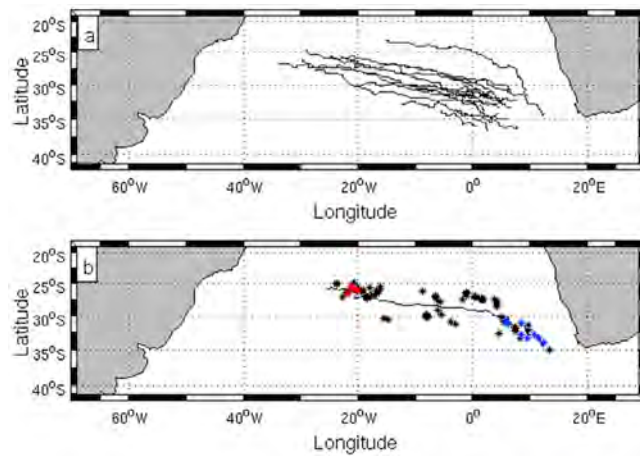


Figure 1. (a) Tracks of the Agulhas rings identified between January 2005 and December 2008 by the automatic algorithm. (b) Map with the track of an eddy first observed in 24 January 2007. The stars represent the position of the 83 ARGO profiles used in the reconstruction of the ring vertical structures. The blue (red) points indicate the position of the ARGO profiles at the beginning (end) of the eddy lifetime that were used to analyze the trapping depth variability.

map with the track of this ring and the positions of the 83 profiles that surveyed its vertical structure. The profiles are observed to span different stages of the eddy life cycle. After fitting the T and S anomaly profiles, obtained by subtracting the ARIVO climatology from the ARGO data, the velocity structure was calculated through the integration of the thermal wind relation with a reference depth of 1500 m. This reference depth was chosen based on the depth limit of the ARGO data and previous work [van Aken *et al.*, 2003]. The dynamic height was calculated using the same reference depth, and is compared with the SLA in Figure 2a. The difference observed in the amplitude is related to the fact that the obtained vertical structure is a representation of the mean over the entire eddy lifetimes, while the SLA represents a time span of 7 days. Moreover, the fitting process smooths the T and S gradients giving rise to smoother dynamical heights. The important point to emphasize is that the eddy shapes are well represented, assuring the fitted sections include the entire region under the influence of the eddies. The resultant eddy vertical structure (Figure 2b) shows a tilted velocity field with a phase difference in relation to the T anomalies. This difference between the velocity and T sections results in a meridional eddy heat flux across the rings trajectories.

[12] In summary, the SLA data was first used to track the Agulhas rings, then to normalize the T and S anomalies

Table 1. General Characteristics of the Agulhas Rings Identified and Tracked Between January 2005 and December 2008, Through the Automatic Algorithm^a

Number of Rings	Duration (days)	Mean Diameter (km)	Mean Amplitude (cm)	Mean Propagation Velocity (m s^{-1})	Number of Profiles
16	497 ± 233	165 ± 69	17 ± 8	0.06 ± 0.02	49 ± 28

^aThe last column shows the number of ARGO float profiles that are available for the reconstruction.

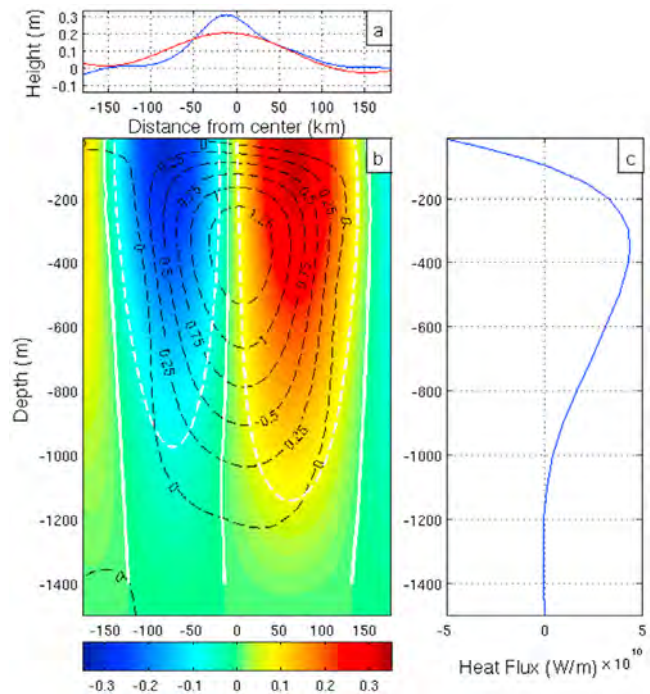


Figure 2. Reconstruction of the ring (first observed in 24 January 2007) vertical structure from the ARGO float profiles: (a) comparison between the AVISO SLA (blue) and the dynamical height (red) relative to 1500 m obtained from the reconstructed density field; (b) eddy vertical structure, where the color contours represent the eddy velocity in m s^{-1} , the black dashed lines the T anomaly, the continuous white lines present the zero velocity horizontal Laplacian used to delimit the eddy influence region for the heat flux calculation, and the dashed white lines indicate the mean water trapping area according to the criteria of Flierl [1981]; (c) meridional heat flux vertical profile obtained from the reconstructed mean vertical structure. A total of 0.02PW northward heat flux across the ring path is obtained by integrating the profile.

from the ARGO profiles used to interpolate the eddy mean structures, and finally to control the quality of the resultant vertical section through the comparison with the calculated dynamical height. The ARGO float profiles provided the necessary information about the vertical structure inside and in the neighborhood of the rings.

3.1. Meridional Heat Flux Estimates

[13] The meridional heat flux profile obtained for the ring first identified in 24 January 2007 (Figure 2c) shows negative (southward) values near the surface, largely compensated by positive (northward) values between the depths of 100 and 1100 m. A resultant heat flux of 0.02 PW northward is obtained by integrating this profile. Assuming that the meridional heat flux is linearly related to the eddy amplitudes and diameters, the equations (2) can be inverted to retrieve the temporal variability of the fluxes obtained from the eddy structures. The mean meridional heat flux obtained along each eddy lifetime is of 0.027 ± 0.014 PW (using all the rings). Consequently, in the study period the Agulhas rings were responsible for an annual eddy meridional heat flux of 0.062 ± 0.012 PW. It is important to emphasize that this heat

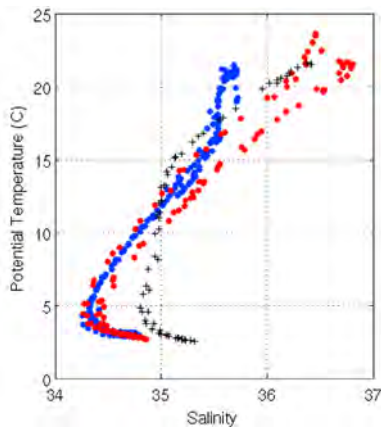


Figure 3. T-S diagram of ARGO float profiles for the Agulhas ring first observed in 24 January 2007, showing the variation of the water properties with the eddy lifetime. The blue points indicate the profiles inside the ring at the beginning (east of 5°E) and the red points at the end (western of 20°W) of its life. The black crosses show the water properties of the ARGO profiles outside the eddy at the end of its lifetime.

flux is not a consequence of the eddies “carrying” trapped water meridionally, but a result of the perturbation of the water column vertical structure along the path of each eddy. Since several eddy paths with different latitudes are considered, this estimation consists of the heat flux across the eddy propagation corridor ($\sim 30^\circ\text{S}$) and not a specific parallel. In addition, if one considers the vertical sections obtained by the reconstruction method as a crude estimate of the real eddy structures close to their first observation dates, an Indian-Atlantic mean heat flux of 0.07 PW is obtained. This estimate is in the range of 0.03–0.08 PW of heat entering the Atlantic Ocean estimated by Gründlingh [1995].

3.2. Volume Transport Estimates

[14] All eddies identified in this study reached the depth of 1500 m, suggesting they should extend deeper than observed by ARGO floats. This agrees with previous observational studies; for example *van Aken et al.* [2003] observed ~ 5000 m deep Agulhas rings. Different eddy vertical structures are expected, as indicated by the different characteristics of the ring tracks. In fact, rings with different vertical structures and a level of no motion near 1000 m were observed by

Garzoli et al. [1999] using ADCPs and hydrographic profiles. From the comparison between the tangential velocities and the eddy propagation velocities it is possible to define the region of trapped water in the ring sections [*Flierl*, 1981]. From the surface ring geometries and the water-trapped region defined in the vertical sections, a mean volume transport of 3.3 ± 2 Sv per eddy was calculated. This value is higher than previous estimates by *Richardson* [2007] (1.3–1.6 Sv) and *Garzoli et al.* [1999] (0.5–2 Sv). The large standard deviation in our result is a consequence of the vertical structure variability between rings.

[15] Since the volume effectively transported by the eddy decreases when the propagation velocity increases, new estimates of the transport can be obtained varying this velocity value. Using the maximum propagation velocities over the whole eddy trajectories to estimate the minimum possible water trapped regions, the mean volume transport decreases to 1.7 ± 1 Sv. Though this value is closer to previous estimates, it should be viewed with care since it combines a mean structure with an instantaneous maximum value of propagation velocity. The difference with the volume transports from previous work are a consequence of the simple cylindrical or conical shapes often adopted for the ring geometry. In the present study the individual eddy shapes are considered. Moreover, while the 1000 m depth is commonly assumed as the limit of the ring [e.g., *Richardson*, 2007; *Dencausse et al.*, 2010], the present results show highly variable trapping depths: between 800 ± 297 m (maximum propagation velocities) and 1133 ± 150 m (mean propagation velocities). The variability in the trapping depth had an important impact in the volume transport calculation. Previous hydrological observations suggest highly variable trapping depths, exceeding 1000 m in some regions [*Gladyshev et al.*, 2008]. Comparing the T and S from the profiles inside the eddy cores at the beginning and at the end of an eddy track (Figure 1b), it is observed that the main modifications in the water properties occur near the surface (Figure 3). This suggests the surface fluxes play a leading role in the modification of the eddy vertical structure. The contrast with the profiles outside the eddy indicates water-trapping depths as high as 1500 m for this particular ring. A strong variability in the trapping depths was observed, with some rings losing their core characteristics as they moved away from the retroflexion region (see auxiliary material).

[16] Assuming the first observation instant as the eddy birth date and combining this information with the mean

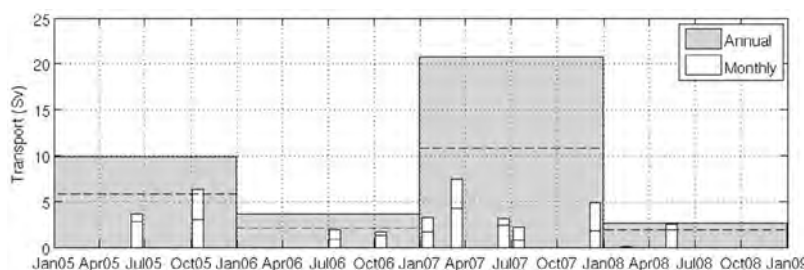


Figure 4. Volume transports by Agulhas rings between 2005 and 2008. The range in the transport bars (dashed lines) correspond to different water trapped regions calculated using the mean and the maximum eddy propagation velocities. The variability in the transport is mainly a function of the variation in the number of rings shed by the Agulhas retroflexion region. Note that there are months without any volume transport estimate, since no rings were observed to be formed during these times.

volume of each observed ring's water trapped region, the annual and monthly volume transports are calculated (Figure 4). The resultant mean values of 9 ± 8 Sv for the mean trapped region, and 5.2 ± 4 Sv for the minimum trapped region, fall in the range calculated by previous work: maximum of 8.5 Sv from Dencausse *et al.* [2010], 10–13 Sv from Richardson [2007] and 6–10 Sv from Garzoli *et al.* [1999]. A striking characteristic of the volume transports presented in Figure 4 is the strong inter-annual variability. The year of 2007 was extreme with volume transport between ~ 11 –21 Sv. The main factor influencing the variability of the volume transport is the number of rings formed per year, though their diameters and vertical structures also played important roles.

4. Conclusions

[17] A method that combines the vertical profiles from the ARGO float program with SSH satellite data was successfully implemented to estimate the Agulhas ring vertical structures. This method enables the characterization of each particular mesoscale structure, allowing better estimates of the eddy meridional heat flux and volume transport. An annual mean meridional heat flux by Agulhas rings of 0.062 ± 0.012 PW northward was obtained. The calculated 0.07 PW heat transported from the Indian Ocean to the Atlantic agrees with previous estimates. Volume transports were calculated for all the rings shed in the period of the study and fell in the range (1.7 ± 1 Sv to 3.3 ± 2 Sv). Though the mean annual volume transport is in the range established by previous work (5.2 ± 4 Sv to 9 ± 8 Sv), a large inter-annual variability was observed. The year of 2007 presented the higher volume transport (11–21 Sv), at least 6 Sv larger than previous values. The variability in the eddy vertical structures was responsible for the standard deviation of the heat flux and volume transport calculations. However, the number of eddies shed per year was of greater importance for the annual flux values.

[18] **Acknowledgments.** The authors would like to thank Bertrand Chapron, Michel Arhan and Pierre-Yves Le Traon for the fruitful discussions we had about this work. We also acknowledge AVISO service website maintained by CLS for making publicly available their sea surface height data. ARGO data were collected and made freely available by the International ARGO Program and the national programs that contribute to it. Special thanks to Robert Scott for the manuscript revision. João M. A. C. Souza was funded through an IFREMER postdoctoral fellowship.

[19] The Editor thanks the two anonymous reviewers for their assistance in evaluating this paper.

References

- Biastoch, A., C. W. Böning, and J. R. E. Lutjeharms (2008), Agulhas leakage dynamics affects decadal variability in Atlantic overturning circulation, *Nature*, *456*, 489–492, doi:10.1038/nature07426.
- Cabanes, C., C. B. Montégut, C. Coatanoan, N. Ferry, C. Pertuisot, K. Von Schuckmann, L. P. Villeon, T. Carval, S. Pouliquen, and P. Y. Le Traon (2010), CORA (CORIOLIS Ocean Database for re-Analyses), a new comprehensive and qualified ocean in-situ dataset from 1900 to 2008 and its use in GLORYS, *CORIOLIS Q. Newsl.*, *37*, 15–19.
- Chaigneau, A., G. Eldin, and B. Dewitte (2009), Eddy activity in the four major upwelling systems from satellite altimetry (1992–2007), *Prog. Oceanogr.*, *83*, 117–123, doi:10.1016/j.pocean.2009.07.012.
- Chelton, D. B., M. G. Schlax, and R. M. Samelson (2011), Global observations of nonlinear mesoscale eddies, *Prog. Oceanogr.*, *91*, 167–216, doi:10.1016/j.pocean.2011.01.002.
- Dencausse, G., M. Arhan, and S. Speich (2010), Routes of Agulhas rings in the southeastern Cape Basin, *Deep Sea Res., Part I*, *57*, 1406–1421, doi:10.1016/j.dsr.2010.07.008.
- Flierl, G. R. (1981), Particle motions in large-amplitude wave fields, *Geophys. Astrophys. Fluid Dyn.*, *18*, 39–74, doi:10.1080/03091928108208773.
- Garzoli, S. L., P. L. Richardson, C. M. D. Rae, D. M. Fratantoni, G. Goni, and A. J. Roubicek (1999), Three Agulhas rings observed during the Benguela Current Experiment, *J. Geophys. Res.*, *104*(C9), 20,971–20,985, doi:10.1029/1999JC900060.
- Gladyshev, S., M. Arhan, A. Sokov, and S. Speich (2008), A hydrographic section from South Africa to the southern limit of the Antarctic Circumpolar Current at the Greenwich meridian, *Deep Sea Res., Part I*, *55*, 1284–1303, doi:10.1016/j.dsr.2008.05.009.
- Gründlingh, M. L. (1995), Tracking eddies in the southeast Atlantic and southwest Indian Ocean with TOPEX/POSEIDON, *J. Geophys. Res.*, *100*(C12), 24,977–24,986, doi:10.1029/95JC01985.
- Le Traon, P. Y., Y. Faugère, F. Hernandez, J. Dorandeu, F. Mertz, and M. Ablain (2003), Can we merge GEOSAT follow-on with TOPEX/POSEIDON and ERS-2 for an improved description of the ocean circulation?, *J. Atmos. Oceanic Technol.*, *20*, 889–895, doi:10.1175/1520-0426(2003)020<0889:CWMGFV>2.0.CO;2.
- Penven, P., V. Echevin, J. Pasapera, F. Colas, and J. Tam (2005), Average circulation, seasonal cycle, and mesoscale dynamics of the Peru Current System: A modeling approach, *J. Geophys. Res.*, *110*, C10021, doi:10.1029/2005JC002945.
- Qiu, B., and S. Chen (2005), Eddy-induced heat transport in the subtropical North Pacific from ARGO, TMI, and altimetry measurements, *J. Phys. Oceanogr.*, *35*, 458–473, doi:10.1175/JPO2696.1.
- Richardson, P. L. (2007), Agulhas leakage into the Atlantic estimated with subsurface floats and surface drifters, *Deep Sea Res., Part I*, *54*, 1361–1389, doi:10.1016/j.dsr.2007.04.010.
- Schmid, C., O. Boebel, W. Zenk, J. R. E. Lutjeharms, S. L. Garzoli, P. L. Richardson, and C. Barron (2003), Early evolution of an Agulhas Ring, *Deep Sea Res., Part II*, *50*, 141–166, doi:10.1016/S0967-0645(02)00382-X.
- Schonten, M. W., W. P. M. de Ruijter, and P. J. van Leeuwen (2000), Translation, decay and splitting of Agulhas rings in the southeastern Atlantic Ocean, *J. Geophys. Res.*, *105*(C9), 21,913–21,925, doi:10.1029/1999JC000046.
- Souza, J. M. A. C., C. de Boyer Montégut, and P. Y. Le Traon (2011), Comparison between three implementations of automatic identification algorithms for the quantification and characterization of mesoscale eddies in the South Atlantic Ocean, *Ocean Sci. Discuss.*, *8*, 483–531, doi:10.5194/osd-8-483-2011.
- van Aken, H. M., A. K. van Veldhoven, C. Veth, W. P. M. Ruijter, P. J. van Leeuwen, S. S. Drijfhout, C. P. Whittle, and M. Rouault (2003), Observations of a young Agulhas ring, Astrid, during MARE in March 2000, *Deep Sea Res., Part II*, *50*, 167–195, doi:10.1016/S0967-0645(02)00383-1.
- van Sebille, E. V., P. J. V. Leeuwen, A. Biastoch, and W. P. M. Ruijter (2010), On the fast decay of Agulhas rings, *J. Geophys. Res.*, *115*, C03010, doi:10.1029/2009JC005585.
- von Schuckmann, K., F. Gaillard, and P. Y. Le Traon (2009), Global hydrographic variability patterns during 2003–2008, *J. Geophys. Res.*, *114*, C09007, doi:10.1029/2008JC005237.

C. Cabanes, DT-INSU, IFREMER, Centre Brest, F-29280 Plouzané CEDEX, France.

C. de Boyer Montégut and J. M. A. C. Souza, Laboratoire d'Océanographie Spatiale, IFREMER, Centre Brest, F-29280 Plouzané CEDEX, France. (jmazeved@ifremer.fr)

P. Klein, Laboratoire de Physique des Océans, IFREMER, Centre Brest, F-29280 Plouzané CEDEX, France.